J Appl Physiol 123: 501–512, 2017.
First published June 1, 2017; doi:10.1152/japplphysiol.00855.2016.

RESEARCH ARTICLE | *Aging and Exercise*

Neuromuscular electrical stimulation improves skeletal muscle regeneration through satellite cell fusion with myofibers in healthy elderly subjects

Ester Sara Di Filippo,[1,2] Rosa Mancinelli,[1,2,3] Mariangela Marrone,[1,2] Christian Doria,[1,2,3] Vittore Verratti,[1,3] Luana Toniolo,[2,4] José Luiz Dantas,[3] Stefania Fulle,[1,2,3] and Tiziana Pietrangelo[1,2,3]

[1]*Department of Neuroscience Imaging and Clinical Sciences, G. d'Annunzio University of Chieti-Pescara, Chieti, Italy;* [2]*Interuniversity Institute of Myology, Italy;* [3]*Laboratory of Functional Evaluation, G. d'Annunzio University of Chieti-Pescara, Chieti, Italy; and* [4]*Department of Biomedical Sciences, University of Padova, Padova, Italy*

Submitted 21 September 2016; accepted in final form 23 May 2017

Di Filippo ES, Mancinelli R, Marrone M, Doria C, Verratti V, Toniolo L, Dantas JL, Fulle S, Pietrangelo T. Neuromuscular electrical stimulation improves skeletal muscle regeneration through satellite cell fusion with myofibers in healthy elderly subjects. *J Appl Physiol* 123: 501–512, 2017. First published June 1, 2017; doi: 10.1152/japplphysiol.00855.2016.—The aim of this study was to determine whether neuromuscular electrical stimulation (NMES) affects skeletal muscle regeneration through a reduction of oxidative status in satellite cells of healthy elderly subjects. Satellite cells from the vastus lateralis skeletal muscle of 12 healthy elderly subjects before and after 8 wk of NMES were allowed to proliferate to provide myogenic populations of adult stem cells [myogenic precursor cells (MPCs)]. These MPCs were then investigated in terms of their proliferation, their basal cytoplasmic free Ca^{2+} concentrations, and their expression of myogenic regulatory factors (*PAX3, PAX7, MYF5, MYOD*, and *MYOG*) and micro-RNAs (miR-1, miR-133a/b, and miR-206). The oxidative status of these MPCs was evaluated through superoxide anion production and superoxide dismutase and glutathione peroxidase activities. On dissected single skeletal myofibers, the nuclei were counted to determine the myonuclear density, the fiber phenotype, cross-sectional area, and tension developed. The MPCs obtained after NMES showed increased proliferation rates along with increased cytoplasmic free Ca^{2+} concentrations and gene expression of *MYOD* and *MYOG* on MPCs. Muscle-specific miR-1, miR-133a/b, and miR-206 were upregulated. This NMES significantly reduced superoxide anion production, along with a trend to reduction of superoxide dismutase activity. The NMES-dependent stimulation of muscle regeneration enhanced satellite cell fusion with mature skeletal fibers. NMES improved the regenerative capacity of skeletal muscle in elderly subjects. Accordingly, the skeletal muscle strength and mobility of NMES-stimulated elderly subjects significantly improved. NMES may thus be further considered for clinical or ageing populations.

NEW & NOTEWORTHY The neuromuscular electrical stimulation (NMES) effect on skeletal muscle regeneration was assessed in healthy elderly subjects for the first time. NMES improved the regenerative capacity of skeletal muscle through increased myogenic precursor cell proliferation and fusion with mature myofibers. The increased cytoplasmic free Ca^{2+} concentration along with *MYOD*, *MYOG*, and micro-RNA upregulation could be related to reduced $O_2^{\cdot -}$ production, which, in turn, favors myogenic regeneration. Accordingly, the skeletal muscle strength of NMES-stimulated lower limbs of healthy elderly subjects improved along with their mobility.

Address for reprint requests and other correspondence: S. Fulle, Dept. of Neuroscience Imaging and Clinical Sciences, G. d'Annunzio Univ. of Chieti-Pescara, Via dei Vestini 31, 66100 Chieti, Italy (e-mail: s.fulle@unich.it).

neuromuscular electrical stimulation; satellite cells; superoxide anion; oxidative status; micro-RNA

ELDERLY PEOPLE experience skeletal muscle frailty, loss of myofibers, and dynapenia (loss of muscle strength), which, in one word, can be defined as sarcopenia. As a consequence, they can experience limited mobility, and, ultimately, mortality. Moreover, sarcopenia can be exacerbated by neurological deficit and/or heavy physical impairment, which, in turn, provoke immobilization. This condition often represents the point of no return in the life of the elderly, because once it is reached, these elderly people cannot perform volitional training, such as endurance or strength training, which has been shown to maintain and increase human skeletal muscle also for the elderly (25, 26, 54, 57).

In this scenario, an effective passive protocol that can be used to induce local skeletal muscle contraction, such as neuromuscular electrical stimulation (NMES), might be particularly useful to counteract the detrimental decline that occurs in sarcopenic muscle. Indeed, it is commonly accepted that NMES can offer advantages over voluntary training for people who have limited ability or are noncompliant for volitional exercise, because of its promotion of specific motor unit recruitment (20).

Effective skeletal fiber contraction involves recruitment and activation of satellite cells in the muscle (57). In vivo, these quiescent satellite cells of postnatal skeletal muscle fibers can be activated to the myogenic precursor cells (MPCs) that are responsible for muscle growth and repair. Although it is currently accepted that this skeletal muscle regeneration can be stimulated by exercise that involves voluntary skeletal muscle contraction, debate still remains as to whether this also occurs for atypical skeletal muscle contraction, such as contraction induced by NMES.

Administration of an electrical current in the microampere range has been successfully used to rescue atrophied mouse muscle (39). Furthermore, different intensities of electrical stimulation (e.g., 2–20 Hz and 0.5–20 mA; 0.3 Hz and 10 μA) can stimulate the proliferation of satellite cells/MPCs and myotube activity and stop the loss of myonuclei in atrophic and damaged mouse skeletal muscle (14, 21, 52). Recently, an NMES protocol was described that is particularly suited to counteract disuse muscle atrophy in men (20). Considering the strict link between atrophy and sarcopenia and the involvement

of MPCs in both of these conditions, we investigated the effects of NMES on myogenesis in elderly human subjects.

We have previously shown that the human regenerative potential of satellite cells derived from skeletal muscle of elderly subjects can be lost through spontaneous increase in the apoptotic commitment of these cells (18). Our previous investigations have suggested that the increased free radical production and oxidative stress that can become established in MPCs from elderly subjects can act as signals for maladaptive phenomena (10, 45, 50). More specifically, accumulation of the superoxide anion ($O_2^{\cdot -}$) is involved in the establishment of oxidative stress in these MPCs (10). This $O_2^{\cdot -}$ is one of the most dangerous oxidant species, and it is mainly produced by mitochondria that have undergone metabolic impairment (37, 51). Here, the key element becomes the amount of $O_2^{\cdot -}$ production and the enzymatic defense that can be adopted by the cells. Indeed, low-intensity training mainly induces a significant $O_2^{\cdot -}$ reduction in MPCs from healthy young muscle (48). However, in some subjects, this training can instead produce a slight $O_2^{\cdot -}$ increase (48). In contrast, in MPCs of elderly subjects, the $O_2^{\cdot -}$ levels and the generic cytosolic oxidation levels are at least one-third more than those in MPCs of young subjects (10). This oxidative stress can provoke extensive cellular damage, apoptosis, and inflammation of skeletal fibers and the satellite cell pool (10, 13, 15, 17). In this scenario, it is important to find stimuli that can be used to reduce the oxidative stress, in order to reduce the signals for inflammation and to promote muscle mass conservation and increased satellite cell stimulation in the elderly.

Some early evidence has demonstrated that NMES can increase intracellular defenses against reactive oxygen species in skeletal muscle of young subjects (20). Moreover, NMES has been shown to promote hypertrophy of the human vastus lateralis skeletal muscle and to increase the maximal force of the quadriceps in young subjects (36). On the basis of this information, we asked whether NMES can influence the regeneration process and the oxidative stress of activated satellite cells (i.e., MPCs) in skeletal muscle of healthy elderly subjects. In particular, we investigated these MPCs in vitro, in terms of their proliferation and differentiation into myotubes and fusion with myofibers, their basal cytoplasmic free Ca^{2+} concentration ($[Ca^{2+}]_{cyt}$), and their gene expression of myogenic regulatory factors (*PAX3*, *PAX7*, *MYF5*, *MYOD*, and *MYOG*) and micro-RNAs (miR-1, miR-133a/b, and miR-206), prior to and following NMES. The oxidative status of these MPCs through $O_2^{\cdot -}$ production and the superoxide dismutase and glutathione peroxidase activities were also investigated. Moreover, the measurement of maximal voluntary contraction in elderly lower limbs permitted us to relate the cellular and molecular adaptation of NMES-stimulated skeletal muscle to the effectiveness of this protocol.

MATERIALS AND METHODS

Subjects

Twelve healthy male elderly subjects [aged 69.5 ± 1.6 (SE)] volunteered to participate in this study. They used to have an active lifestyle but were not engaged in any specific exercise-training protocols (≥6 mo) before their enrollment in this study. One week before and 2 days after the NMES sessions, these subjects had their height, weight, and body fat measured, and their body mass index was calculated. Their bilateral isometric maximal voluntary contraction (MVC) of the lower limbs was measured using a leg extension device (Nessfit, San Giovanni Teatino, Italy) that was equipped with a loading cell to measure the strength output (Globus, Codognè, Italy). The subjects remained in a seated position on the leg extension device with their knees at 90°, and they performed an MVC for 5 s using both legs. The test was performed three times, and the recovery time between tests was 2 min. The highest value recorded was used as the MVC (46).

Functional Assessment and Tiny Percutaneous Needle Biopsy

Five-times-sit-to-stand test. The five-times-sit-to-stand test (FTSST) was applied as described in a previous study using a 43-cm-high chair. After a signal from the evaluator, the volunteers stood up and sat down five times as quickly as possible, maintaining their arms crossed on their chest. Before the test, the evaluator provided instructions to the volunteers for a standardized execution: *1*) "You need to maintain your arms crossed on your chest during the entire test"; *2*) "you need to stand up and sit down five times as quickly as you can when I say 'Go'"; *3*) "the test begins when I say 'Go' and stops when you completely touch the chair on the fifth repetition"; and *4*) "you need to stand up fully and touch the chair in every repetition, but you should not touch your back to chair backrest during the test" (58). Volunteers performed the FTSST three times. The first set consisted of a submaximal performance for test familiarization. The final two sets were performed to calculate the reliability and typical error of the FTSST, the best performance being considered for the analyses.

Timed-up-and-go test. The timed-up-and-go test (TUG) was applied as described in a previous study (48a). The volunteers were required to stand up, walk 3 m, turn, walk back, and sit down. Time to complete this task was the performance variable, evaluating mobility capacity. Two evaluators were positioned on opposite sides of the walking course (one between 0 and 1.5 m and another between 1.5 and 3.0 m) to avoid any serious consequences in the case of a fall. As in the FTSST, the volunteers performed the TUG three times for familiarization and reliability purposes.

One day after the functional test, the tiny percutaneous needle biopsies of the vastus lateralis muscles were performed. The biopsy of the vastus lateralis muscle was performed at a level about one-third of the distance from the upper margin of the patella to the trochanter major. The choice of this position was motivated by the anatomical consideration that the area lacks significant neurovascular structures. For this reason the tiny percutaneous needle biopsy procedure was well tolerated. More detailed information has been extensively described by Pietrangelo et al. (43, 47).

This study was approved by the Ethics Committee of the G. d'Annunzio University of Chieti-Pescara, Italy (protocol nos. 1233/06 and 1884 COET), and it was conducted according to the Helsinki Declaration. All of the subjects who participated signed their informed consent.

Neuromuscular Electrical Stimulation Sessions

The NMES protocol consisted of a training program that lasted 18 min. The 12 subjects performed 40 passive isometric bilateral contractions that were stimulated by a NMES device (Genesy 1200 Pro; Globus). This was applied for three sessions per week over an 8-wk period. During the NMES session, the subjects were seated on a leg extension machine (NSFT 07036; Nessfit) with the knee joint fixed at 90° knee extension, to provide the isometric condition during the stimulation. Two active electrodes (contact area, 25 cm^2) were positioned over the motor points of the quadriceps muscles, as close as possible to the motor point of the vastus lateralis and vastus medialis muscles. A dispersive electrode (contact area, 50 cm^2) was placed 5–7 cm below the inguinal crease, close to the stimulation loop. Rectangular-wave pulse currents (75 Hz every 400 μs) were delivered with a rise time of 1.5 s, a steady tetanic stimulation time of 4 s, and a fall

time of 0.75 s (total duration of contraction, 6.25 s). A rest interval of 20 s was provided between stimulations. The intensity was monitored and recorded for each 5-min period. The intensity of the NMES was gradually increased to an individual maximally tolerable intensity, which corresponded to the pain threshold of each subject. The subjects were motivated to adjust their intensity during the training session to maintain the maximum tolerable intensity throughout the session, reaching an intensity of 40 ± 16 mA at the end of the training period.

Satellite Cell Population and Myogenicity

A part of the tiny percutaneous muscle biopsies (~10 mg) was treated to obtain the muscle cells (43). The progeny of in vitro satellite cells, MPCs, were initially expanded in growth medium and differentiated into myotubes as previously described (16, 45, 48). These MPCs from the vastus lateralis of the 12 healthy elderly subjects were obtained before the NMES sessions were started and after they were completed, with these samples defined as pre-NMES and post-NMES, respectively.

Briefly, the percentages of myogenicity were obtained by counting the MPCs that were positive for an antibody against desmin (16), with respect to all of the cells present in the field of view. We counted 6,341 and 6,369 cells in pre- and post-NMES samples, respectively. At a confluence of 70–80%, the cells were split, and the population-doubling level (PDL) was calculated. This is given by the ratio between the number of cells that were detached (Nd) with respect to the number of cells that were initially seeded (Ns; i.e., Nd/Ns), and log Nd/Ns was calculated and divided by ln 2. The MPC controls derived from tiny percutaneous needle biopsy samples of subjects without NMES were analyzed as previously described.

The differentiation of these MPCs into myotubes was measured in terms of the multinucleated cells that were positive to the primary antibody against myosin heavy chain after 7 days of differentiation. This is reported as the fusion index, as a percentage defined by counting the number of nuclei present in the myotubes, with respect to the total number of nuclei in the observed field (i.e., nuclei in myotubes/total nuclei × 100%). Myotubes were defined as those that were positive to the primary antibody against myosin heavy chain and that had at least two nuclei (48). We counted 2,717 and 2,731 cells in pre- and post-NMES samples, respectively. Moreover, in the samples that were differentiated for 7 days, the number of mononucleated desmin$^+$ cells was counted, which represents the number of myogenic cells that were not able to fuse into multinucleated myotubes. We counted 2,150 and 2,139 cells in pre- and post-NMES samples, respectively.

Myonuclear Density of Single Myofibers

Another part of the tiny percutaneous muscle biopsies (~5 mg) from four of these subjects was manually dissected to obtain single skeletal myofibers (47). The myonuclei along these single myofibers were counted, to determine the nuclear domain. Briefly, to localize the nuclei, single myofibers were stained with 4′,6-diamidino-2-phenylindole (DAPI; 25 μg/ml; Sigma-Aldrich) for 10 min. To precisely measure the volume, the fibers have been stained with monoclonal mouse antibody anti-α-actinin (clone EA-53; Sigma-Aldrich). The myonuclear density was determined as the number of nuclei in a constant myofiber volume (10^6 μm^3). A confocal microscope (Vico; Nikon) was used to acquire the fluorescent images (32, 40).

Mechanical Features and Phenotype of Single Fibers

Muscle biopsy fragments for single fibers were stored at −20°C and analyzed within 2 wk of sampling. The biopsies were stored in skinning solution with 50% (vol/vol) glycerol until the day of the experiment. This solution contains a high-potassium and high-EGTA concentration that depolarizes membranes, removes calcium, and induces a rigor to ensuring optimal conditions for fiber preservation. Before the analysis, the skinning-glycerol mixture was replaced with ice-cold skinning solution containing ATP, to induce fiber relaxation. From each biopsy, single fibers were manually dissected using a stereomicroscope (×10–60 magnification). Following dissection, fibers were bathed for 10 min in skinning solution containing 1% (vol/vol) Triton X-100 to completely have the membranes in solution. Fiber segments of 1–2 mm in length were cut, and light aluminum clips were applied at both ends. Then they were transferred to the experimental apparatus, and cross-sectional area (CSA) and tension development during maximal calcium-activated isometric contractions at 12°C were measured according to a previously described procedure (41, 56). At the end of the experiment, each fiber was collected and put in Laemmli solution for electrophoretic analysis (see below). All solutions employed for single-fiber experiments were prepared as described previously (7).

Electrophoretic Separation and Quantification of Myosin Heavy Chain Isoforms

The fibers were characterized for their myosin heavy chain (MHC) isoform. Muscle biopsy fragments were solubilized in an appropriate volume of Laemmli solution [Tris 62.5 mM, glycerol 10% (vol/vol), SDS 2.3% (wt/vol), and β-mercaptoethanol 5% (vol/vol), with E-64 0.1% (wt/vol) and leupeptin 0.1% (wt/vol) as antiproteolytic factors; pH 6.8] and stored at −80°C until the analysis. Appropriate amounts (~10 μg total protein/lane) of the protein suspension were diluted in loading buffer (Laemmli solution with 0.01% bromophenol blue) and boiled for 5 min at 80°C before loading onto polyacrylamide gels. Separation of MHC isoforms was performed on 8% (wt/vol) gels (18 cm × 16 cm × 1 mm) at 70 V for 1.5 h and at 230 V for a further time according to the guidelines of Talmadge and Roy (55a). The gels were stained with Coomassie blue dye. After staining, three separate bands were detected in the 200-kDa region, corresponding to MHC I, IIA, and IIX, in order of migration from fastest to slowest. For each biopsy sample fragment, at least two independent electrophoretic runs were performed. Gel patterns were digitized with an HP Scanjet G4050 at a resolution of 1,200 dpi. The myosin isoform distribution was achieved by densitometric analyses of the bands after staining with Coomassie blue. Each band was characterized by a value of the

Table 1. *Anthropometric characteristics, isometric maximal voluntary contraction of lower limb, and functional performance measured in healthy elderly subjects before and after the neuromuscular electrical stimulation protocol*

	NMES		Control	
Characteristic	Pre	Post	Pre	Post
Weight, kg	74.2 ± 6.9	74.5 ± 7.0	76.8 ± 4.2	77.5 ± 4.0
Height, m	1.65 ± 0.06	1.65 ± 0.06	1.66 ± 0.03	1.66 ± 0.03
BMI, kg/m^2	27.3 ± 2.7	27.4 ± 2.8	27.9 ± 2.2	28.2 ± 2.1
Body fat, %	26.7 ± 5.1	25.6 ± 5.2	24.8 ± 3.5	24.7 ± 3.6
MVC, N	546 ± 126	605 ± 118*	499 ± 137	488 ± 125
FSST, s	7.96 ± 0.71	6.50 ± 0.30**	7.55 ± 0.98	7.43 ± 1.14
TUG, s	6.02 ± 1.15	4.71 ± 0.51#	5.33 ± 0.52	5.45 ± 0.49

Values are means ± SD. BMI, body mass index; NMES, neuromuscular electrical stimulation protocol; MVC, maximal voluntary contraction; FSST, five-times-sit-to-stand test; Pre and Post, before and after NMES, respectively; TUG, timed-up-and-go test. *Significant difference for interaction time × group for NMES (n = 14) vs. control (n = 8) group [F(1.264,2.574) = 5.014; P = 0.037; np^2 = 0.200; 1 − β = 0.568]. **Significant difference between Pre and Post for NMES group [n = 5; F(4.056,1.962) = 24.811; P = 0.001; np^2 = 0.674; 1 − β = 0.995] and interaction time × group for NMES (n = 5) vs. control (n = 9) group [F(2.866,1.962) = 17.529; P = 0.001; np^2 = 0.594; 1 − β = 0.969]. #Significant difference between Pre and Post for NMES group [n = 4; F(1.972,1.289) = 16.823; P = 0.002; np^2 = 0.605; 1 − β = 0.961] and interaction time × group for NMES (n = 4) vs. control (n = 9) group [F(2.818,1.289) = 24.044; P = 0.001; np^2 = 0.686; 1 − β = 0.993].

Table 2. *Myogenicity and differentiation features of MPCs isolated from the vastus lateralis of healthy elderly subjects before and after the NMES sessions*

	Myogenicity,	Differentiation	
Condition	% Desmin$^+$	Fusion Index, %	Desmin$^+$ Unfused, %
Pre-NMES	64.9 ± 4.5	46.7 ± 6.9	57.0 ± 9.6
Post-NMES	71.1 ± 5.4	50.7 ± 6.2	50.7 ± 8.6

Values are means ± SE. Pre- and post-NMES, before and after the NMES sessions.

brightness-area product (BAP), after black/white inversion employing Li-Cor Image Studio Lite (version 5.0). From each line, BAP values for the bands identified as MHC isoforms were summed, the BAP value for each isoform was expressed as a percentage of the total, and the mean values of myosin isoform distribution for all subjects were obtained. The reproducibility of the procedure was confirmed by calculating isoform ratios of selected samples from gels loaded with different amounts of such samples.

Intracellular Calcium Concentrations

The MPCs were loaded with fura-2 AM (final concentration, 5 μM) for 30 min, washed by gentle solution removal, and incubated for a further 30 min at 37°C prior to the $[Ca^{2+}]_{cyt}$ measurements, to allow intracellular fura-2 AM deesterification (27). The experiments were performed and images were acquired using the procedures and setup described by Pietrangelo et al. (44). Thapsigargin (1 μM; cat. no. T9033; Sigma-Aldrich), a known releaser of internal Ca^{2+} stores, was added in the MPCs to induce the emptying of the intracellular Ca^{2+} stores. The thapsigargin-dependent $[Ca^{2+}]_{cyt}$ transients were recorded for at least 2 min, and analysis of the area under the 2-min transients was performed using the specific "area under the curve" function of GraphPad Prism software, version 5 (GraphPad Software, La Jolla, CA).

Reactive Oxygen Species

Superoxide anion ($O_2^{\cdot -}$) levels were determined using the conventional assay based on the dye nitro blue tetrazolium chloride (cat. no. N6639; Sigma-Aldrich), which is reduced to formazan by $O_2^{\cdot -}$, determined at 550 nm using a fluorometer (SPECTRAmax Gemini XS; Molecular Devices, Toronto, ON, Canada; 10, 48).

The cellular oxidant levels were determined using the dye 2,7-dichlorofluorescein diacetate (DCF; cat. no. D6883; Sigma-Aldrich). The fluorescence was determined at 530 nm (excitation, 490 nm) using a fluorometer (SPECTRAmax Gemini XS; Molecular Devices), with the data analyzed using SOFTmax Pro software (48).

Antioxidant Enzyme Activity

The antioxidant enzyme activities of superoxide dismutase and glutathione peroxidase (53, 55) were analyzed for the cytosolic fractions of undifferentiated MPCs. The superoxide dismutase activity, where 2 $O_2^{\cdot -}$ (+ 2 H^+) is oxidized to form O_2 and H_2O_2, was determined as previously described (48). The glutathione peroxidase enzymatic activity was determined according to Shakirzyanova et al. (53) and reported as specific activities.

Western-Blotting Analysis

Western-blotting analysis was performed on 40-μg lysates from pre- and post-NMES MPCs, using superoxide dismutase type 1 (SOD1; 71G8) mouse monoclonal antibody (mAb; no. 4266; Cell Signaling Technology, Danvers, MA) at 1:1,000, SOD2 (D9V9C) rabbit mAb (no. 13194; Cell Signaling Technology) at 1:1,000, and β-actin (8H10D10) mouse mAb (no. 3700; Cell Signaling Technology) at 1:1,000, as primary antibody. Secondary horseradish peroxidase-conjugated antibodies (Cell Signaling Technology) were used at 1:5,000. Bands were detected and pictured at Bio-Rad GelDoc by LiteAblot Plus enhanced chemiluminescent substrate (EuroClone); densitometry analyses were performed with ImageJ software (10).

Quantitative Real-Time PCR for Myogenic Transcriptional Factors and miRNAs

The RNA was extracted from the MPCs using PureLink RNA mini kits (Invitrogen, Life Technologies), as described by Di Filippo et al. (10). Briefly, 500 ng of extracted RNA were reverse transcribed using Superscript III First-Strand Synthesis SuperMix kits (Invitrogen, Life Technologies). Quantitative real-time PCR was performed on 1:5 diluted cDNA, using Platinum SYBRgreen SuperMix-UDG (Invitrogen, Life Technologies). The myogenic regulatory factors investigated were *PAX3, PAX7, MYF5, MYOD*, and *MYOG*. GAPDH was used as the housekeeping gene, and the data are shown as difference in cycle threshold (ΔCt).

PureLink miRNA isolation kits were used for the miRNA extractions (cat. no. K1570-01; Invitrogen, Life Technologies, Molecular Devices, Sunnyvale, CA), according to Di Filippo et al. (10). The relative quantification of the miRNA targets was performed using the ΔCt formula. The specific miRNA sequence probes used have the following catalog numbers: hsa-miR-16-5p, no. 000391; hsa-miR-1, no. 002222; hsa-miR-206, no. 000510; hsa-miR-133b, no. 002247; and hsa-miR-133a, no. 002246. miR-16 was used as the housekeeping gene, and the data are shown as ΔCt. Three independent experiments were performed, each performed in triplicate.

Statistical Analysis

The statistical analysis was performed using GraphPad Prism software, version 5. The data are reported as means ± SE unless

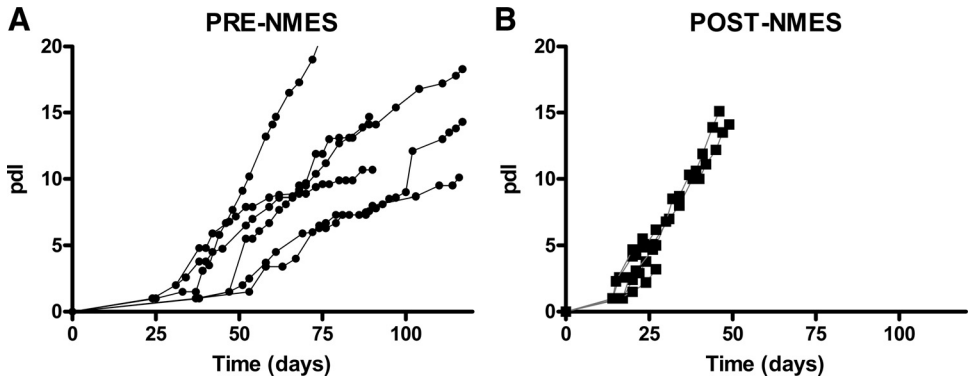

Fig. 1. Population-doubling level of MPCs. Population-doubling levels of MPCs (undifferentiated cells) obtained from the skeletal muscle of six representative healthy elderly subjects, with respect to the days of in vitro cultivation of these cells, as pre-NMES (*A*) and post-NMES (*B*).

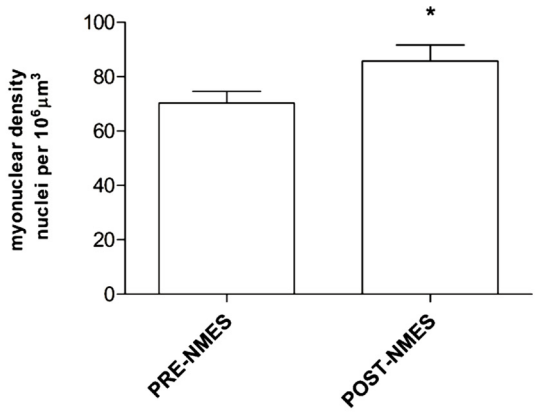

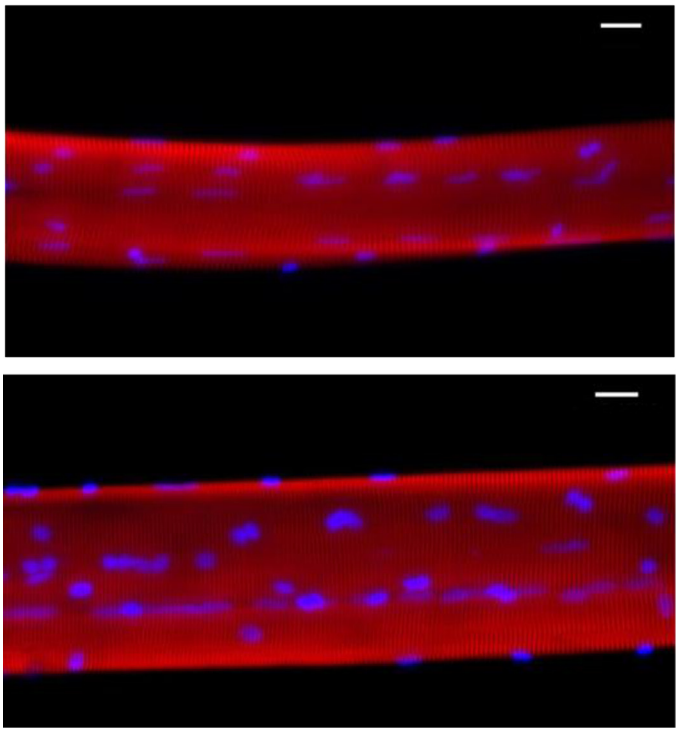

Fig. 2. Myonuclei fused with single mature myofibers. The graph shows the numbers of myonuclei counted for the single dissected myofibers from the muscle needle biopsy of elderly subjects (per 10^6 μm^3 myofiber volume). The myofibers analyzed were 27 and 33 for pre- and post-NMES samples, respectively. The images show an example of human fibers stained for determination of myonuclear density: the nuclei are revealed with DAPI; an antibody against α-actinin allows us to determine the volume. *Top*: image of pre-NMES myofiber. *Bottom*: image of post-NMES myofiber. Scale bar, 20 μm. $*P \leq 0.05$.

otherwise indicated. Unpaired and paired *t*-tests were used to reveal statistical differences between cellular populations and single myofiber analysis, respectively, at pre- and post-NMES.

Mixed analysis of variance (mixed ANOVA) was used to analyze differences between groups and over time (control vs. NMES-stimulated elderly) in addition to Bonferroni post hoc comparisons. Significance is indicated as $*P \leq 0.05$, $**P \leq 0.005$, and $***P \leq 0.0001$.

RESULTS

Maximal Voluntary Contraction in Elderly Subjects

The anthropometric characteristics of the 12 healthy elderly subjects who participated in the NMES sessions did not vary significantly (Table 1). However, compared with the pre-NMES maximal voluntary contractions, the post-NMES values showed a significant increase as well as the FTSST and TUG (Table 1).

Myogenic Characteristics and Analysis of MPC Differentiation

The myogenic characteristics of the MPCs are reported in Table 2. Here, from pre-NMES to post-NMES, there were no significant differences in the MPC myogenicity (i.e., number of desmin$^+$ cells), fusion index, and desmin$^+$ unfused MPCs at 7 days of differentiation, as for control samples (data not shown).

Proliferation Rate In Vitro

The PDLs of the pre-NMES and post-NMES MPCs were calculated at each passage, when the cells reached ~80% confluence. As can be seen in Fig. 1, the pre-NMES MPCs reached 10 PDL in 50–120 days (Fig. 1*A*), whereas the post-NMES MPCs of the same subjects reached the same PDL in 30–35 days (Fig. 1*B*), demonstrating an increased rate of MPC proliferation post-NMES, similar for all subjects. The MPC controls, without NMES stimulation, reached 10 PDL in 50–80 days, showing a similar proliferation trend of pre-NMES MPCs (data not shown).

Myonuclear Density on Single Mature Myofibers

The single mature myofibers showed significant increases from pre-NMES to post-NMES for the myonuclei fused to the myofibers ($P \leq 0.05$; Fig. 2).

MHC Fiber Phenotype

The fiber type composition of the vastus lateralis muscle was determined by analyzing the proportion of slow (MHC I) and fast (MHC IIA and IIX) myosin heavy chain isoforms in pre- and post-NMES biopsy samples. The average percentage of fibers that express the specific MHC isoform is shown in Fig. 3. In our sample, slow MHC I fibers were significantly increased in post-NMES compared with pre-NMES ($P \leq 0.05$). The percentage of fast MHC IIA fibers did not significantly vary, whereas that of MHC IIX ones showed a decrease that was not statistically significant.

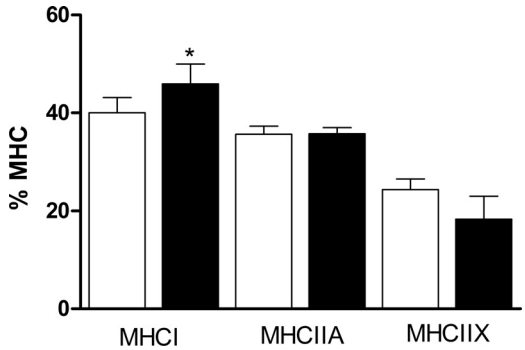

Fig. 3. MHC isoform distribution in biopsy samples collected before and after NMES. The MHC isoform distribution was determined by electrophoretic separation and densitometric analysis of proteins of biopsy samples from the vastus lateralis muscle. The dark columns represent the percentages of the MHC isoform distribution post-NMES, and the white columns represent pre-NMES percentages. $*P \leq 0.05$.

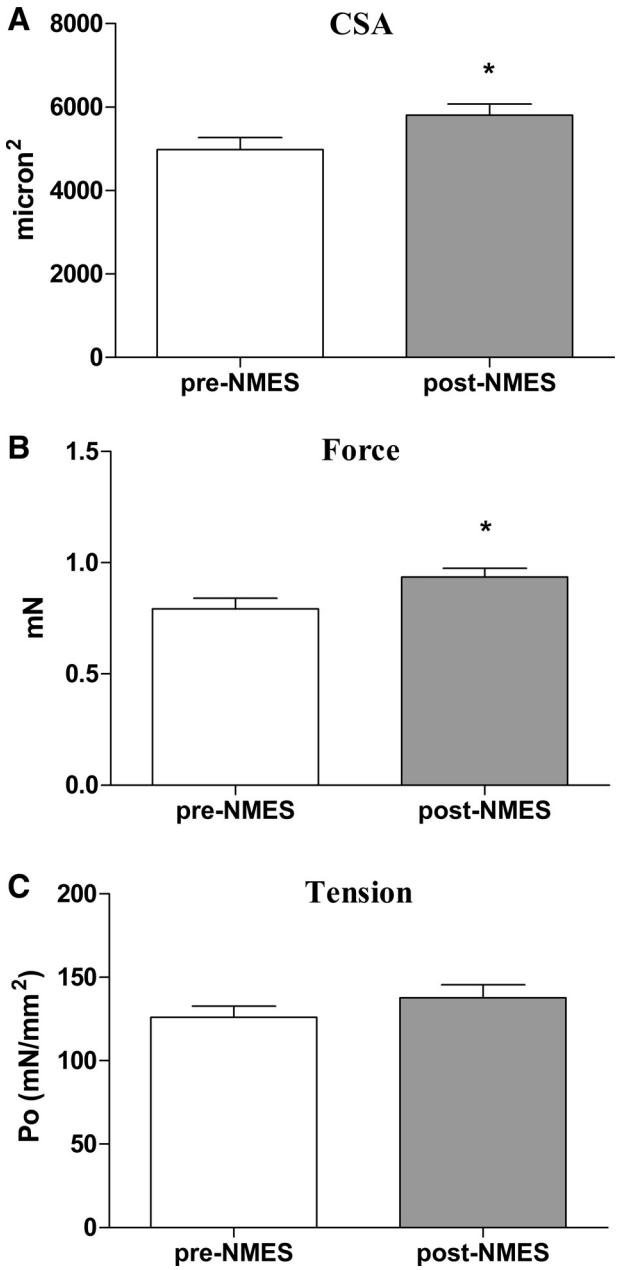

Fig. 4. Phenotype and isometric tension of single fiber. Single-fiber analysis: cross-sectional area (*A*), force (*B*), and specific isometric tension (*C*). The white and dark columns represent pre-NMES and post-NMES samples, respectively. *A*: cross-sectional area (CSA) of single muscle fibers obtained from the vastus lateralis. *B:* force developed by single fiber. *C*: reported measurements of specific isometric tension (force/CSA) developed in maximal calcium-activated contraction by the same fibers. $*P \leq 0.05$.

Muscle Fiber Cross-Sectional Area and Specific Tension

The results on single muscle fibers ($n = 80$) are displayed in Fig. 4. The CSA was significantly incremented at post-NMES vs. pre-NMES (5,810 ± 267 vs. 4,983 ± 288 μm^2, $P \leq 0.05$). The average force (F_o) significantly increased ~20%, from 1.06 ± 0.06 to 1.25 ± 0.05 mN in post-NMES ($P \leq 0.05$).

The value of specific tension (P_o), the isometric strength per unit of fiber area (F_o/CSA), was 126.0 ± 6.7 and 137.8 ± 7.7 mN/mm^2 in pre- and post-NMES, respectively. Although P_o tended to increase, this increment was not statistically significant.

Cytoplasmic Free Ca^{2+} Concentrations of Undifferentiated MPCs

The basal $[Ca^{2+}]_{cyt}$ was significantly increased in the undifferentiated MPCs from pre-NMES to post-NMES ($P \leq 0.05$; Fig. 5*A*). Analysis of the time courses of the Ca^{2+} released from the intracellular stores by thapsigargin (Fig. 5*B*) dem-

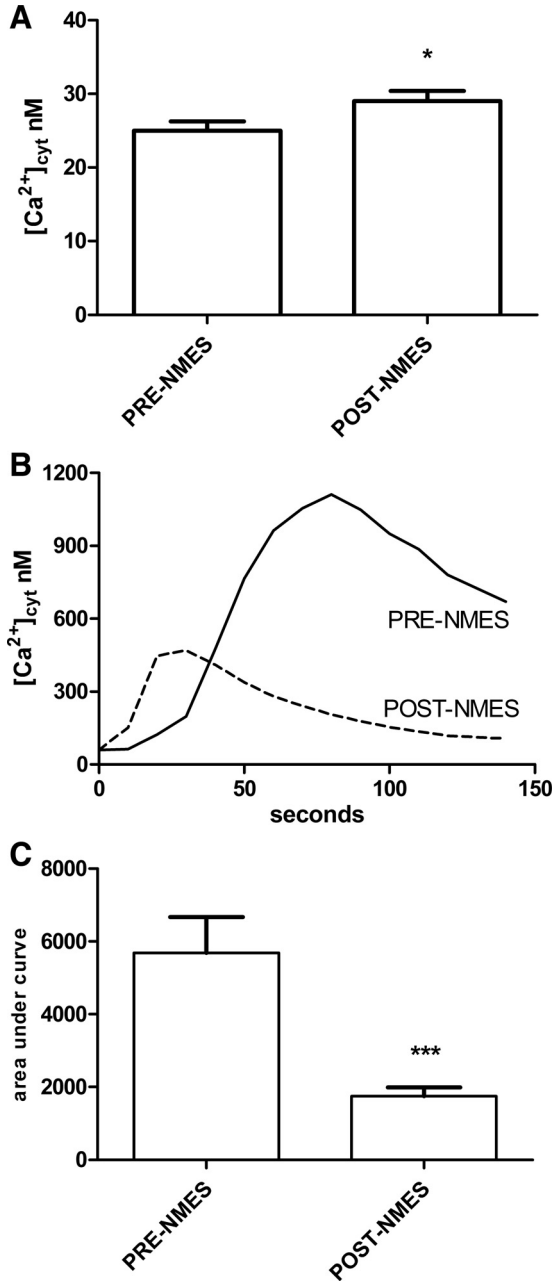

Fig. 5. Free intracellular Ca^{2+} concentrations of MPCs. *A*: free cytoplasmic Ca^{2+} concentrations of the undifferentiated MPCs pre-NMES and post-NMES, as the basal $[Ca^{2+}]_{cyt}$. $*P \leq 0.05$. *B*: time course of the thapsigargin-dependent Ca^{2+} release. *C*: area-under-the-curve measures for the $[Ca^{2+}]_{cyt}$ of the undifferentiated MPCs pre-NMES and post-NMES, for estimation of the thapsigargin-sensitive Ca^{2+} stores released over the first 2 min of thapsigargin stimulation. $***P \leq 0.0001$.

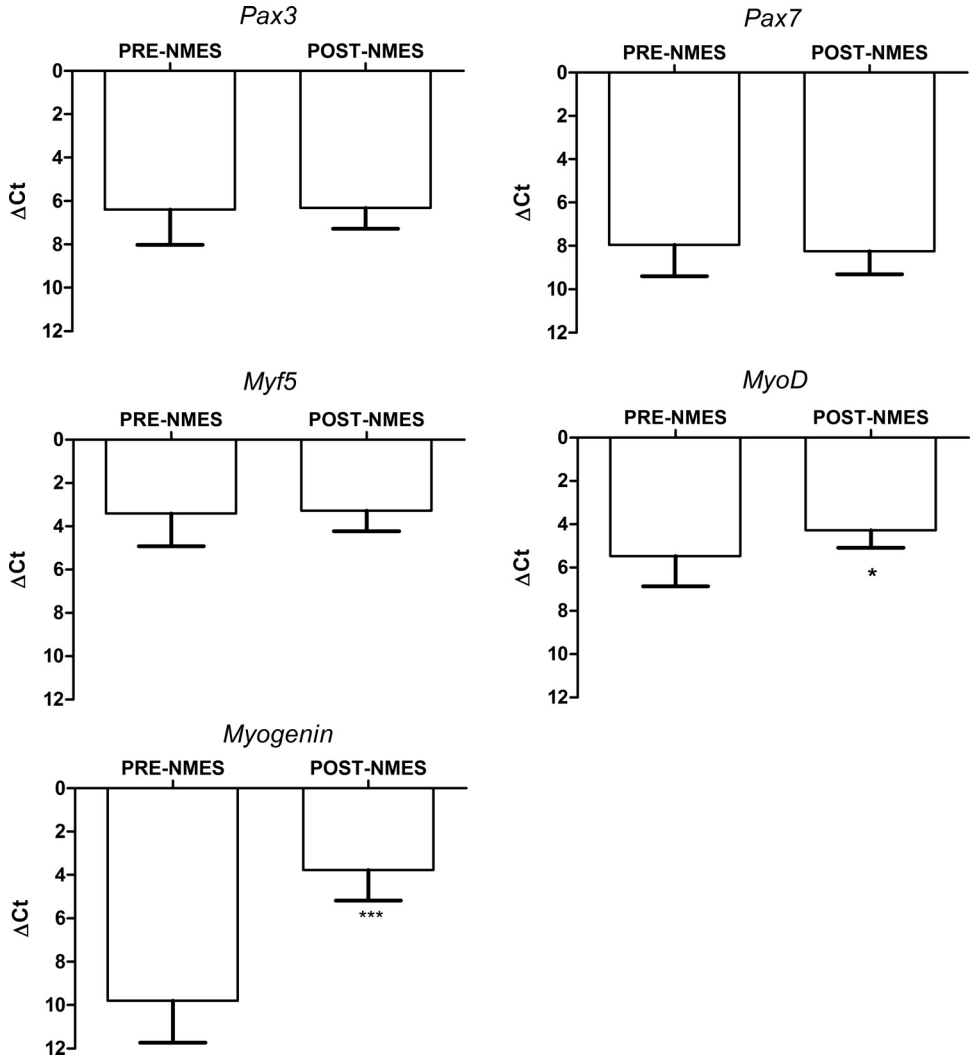

Fig. 6. Gene expression of early transcriptional and myogenic regulatory factors. Pre-NMES to post-NMES mRNA expression levels (as ΔCt) for *PAX3*, *PAX7*, *MYF5*, *MYOD*, and myogenin gene expression. Data are means ± SE from three independent experiments, each performed in triplicate. $*P \leq 0.05$, $***P \leq 0.0001$.

onstrated that in these undifferentiated MPCs, from pre-NMES to post-NMES, there was less Ca^{2+} released. The analysis of the area under the curve for these thapsigargin-dependent $[Ca^{2+}]_{cyt}$ changes from pre-NMES to post-NMES showed a significant reduction ($P \leq 0.001$; Fig. 5*C*).

Myogenic Regulatory Factor Gene Expression Profiles

For the undifferentiated MPCs, from pre-NMES to post-NMES, the myogenic transcription factors *PAX3, PAX7*, and *MYF5* did not change their expression levels, whereas *MYOD*

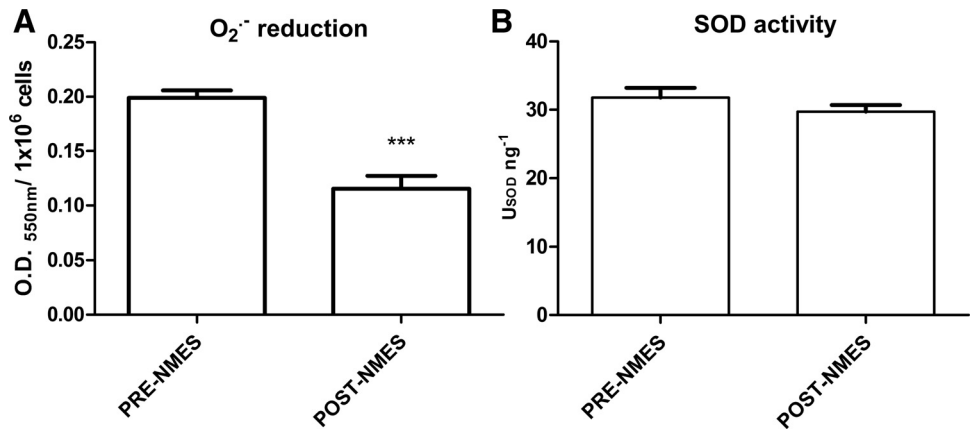

Fig. 7. Superoxide anion production and superoxide enzymatic dismutation. Quantitative analyses from pre-NMES to post-NMES in MPCs for $O_2^{\cdot-}$ (*A*) and the activity of the enzyme superoxide dismutase (SOD; *B*). The SOD units (U_{SOD}) were calculated considering that 1 SOD unit is defined as the quantity that inhibits the rate of cytochrome *c* reduction by 50% per nanogram of protein (*B*). $***P \leq 0.0001$. O.D., optical density.

and *MYOG* were significantly upregulated ($P \leq 0.05$ and $P \leq 0.0001$, respectively; Fig. 6).

Superoxide Anion Production and Basal Levels of Oxidant Species

The undifferentiated MPCs from pre-NMES to post-NMES showed significant $O_2^{\cdot -}$ decrease (by ~40%; Fig. 7*A*).

The DCF fluorescence did not vary significantly from pre-NMES to post-NMES (data not shown).

Antioxidant Enzyme Activity

The activity of the cytosolic fractions from pre-NMES to post-NMES for the antioxidant enzyme superoxide dismutase showed a decreasing trend (31.8 ± 1.4 vs. 29.7 ± 1 U superoxide dismutase/ng; Fig. 7*B*). In contrast, the glutathione peroxidase enzymatic activity remained the same from pre-NMES to post-NMES (0.25 ± 0.06 vs. 0.27 ± 0.05, data not shown).

SOD1 and SOD2 Protein Expression

Representative SOD1 and SOD2 bands obtained by MPCs at pre- and post-NMES are shown in Fig. 8*A*. The amounts of both SOD mitochondrial type 2 and SOD cytosolic type 1 are reported in Fig. 8, *B* and *C*, by Western-blotting analysis.

Epigenetic miRNA Profile

Analysis of the miRNA expression from pre-NMES to post-NMES showed significant upregulation of miR-1, miR-133a, miR-133b, and miR-206 ($P \leq 0.0001$; Fig. 9).

DISCUSSION

The lowered regenerative potential of satellite cells that occurs during human ageing is known to be linked to the accumulation of oxidant species such as $O_2^{\cdot -}$, together with inadequate scavenger activity. These effects provoke cellular damage and impair the ability of satellite cells to efficiently divide into the MPCs that can differentiate to sustain muscle mass and function (5, 10, 12, 16, 30, 45). The hypothesis for the present study was that NMES positively stimulates skeletal muscle regeneration of healthy elderly subjects through a reduction in the MPC oxidation levels.

The data here for the MPC populations obtained after the NMES (i.e., post-NMES) suggest that this procedure can promote increased proliferation rate along with increased fusion of these adult stem cells with the existing myofibers.

We investigated some of the potential molecular aspects as key elements of this regeneration process, in terms of $[Ca^{2+}]_{cyt}$ homeostasis, muscle-regulating transcription factors and miRNA expression, and oxidative species management.

In these undifferentiated MPCs, these data showed a post-NMES reduction in the $[Ca^{2+}]_{cyt}$ of the (thapsigargin-releasable) intracellular Ca^{2+} stores in favor of an increase in basal $[Ca^{2+}]_{cyt}$. This is in line with the increased ability of these post-NMES MPCs to fuse with existing myofibers (6, 27, 29). Release of the free Ca^{2+} from intracellular stores occurs during the early steps of myoblast differentiation (3), when a proliferative boost is required (33, 42). On this basis, our data confirm the increased proliferation rate in the post-NMES MPCs. The NMES-dependent $[Ca^{2+}]_{cyt}$ increase might influence the fusion process via two key Ca^{2+}-dependent enzymes, the transcription factor nuclear factor of activated T cells (NFAT) and the protein kinase CamKII, which stimulate myogenin (2). Indeed, an increase in $[Ca^{2+}]_{cyt}$ is required for activation of myogenic transcription factors, such as myogenin (1). Accordingly, myogenin gene expression was significantly upregulated here. It is also worth mentioning that this gene was not linked to myotube formation, because the fusion index was similar here between the pre-NMES and post-NMES MPCs, although we believe that it is instrumental for MPC fusion with existing myofibers. Indeed, the post-NMES MPCs showed increased proliferation rate along with no *MYF5, PAX3*, and *PAX7* variation but *MYOD* overexpression with respect to pre-NMES MPCs. It has been extensively demonstrated that this specific transcription factor regulation occurs when MPCs are committed to fusion escaping the self-renewal (8).

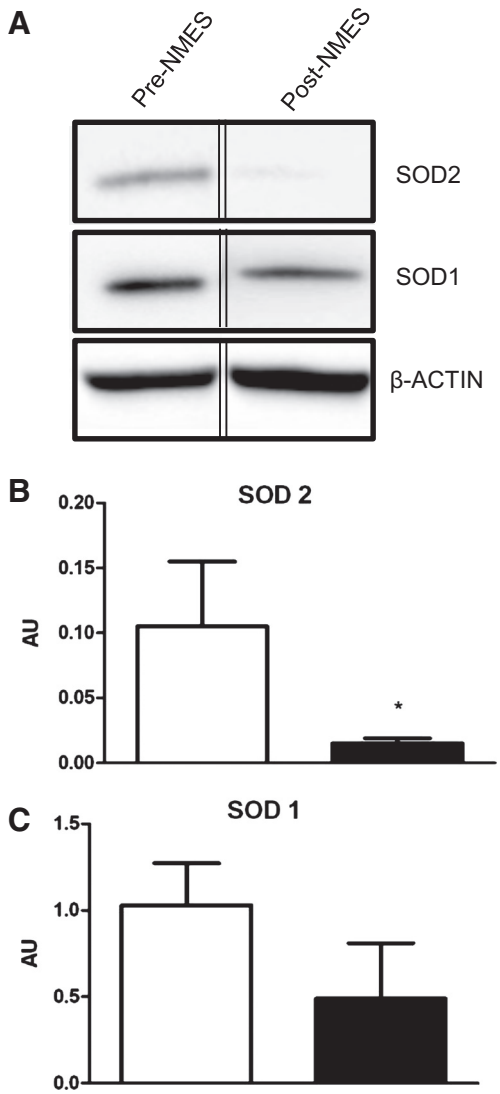

Fig. 8. SOD1 and SOD2 protein expression. Western-blotting analysis of superoxide enzymes cytosolic type 1, and mitochondrial type 2. *A*: representative bands of SOD1 and SOD2 enzymes obtained by MPCs from vastus lateralis muscle biopsies before (pre-) and after (post-) NMES. *B* and *C*: SOD2 and SOD1 protein quantification. *$P \leq 0.05$; $n = 4$. AU, arbitrary units.

Considering the importance of oxidative stress in human satellite cells and its role in impairment of regenerative pro-

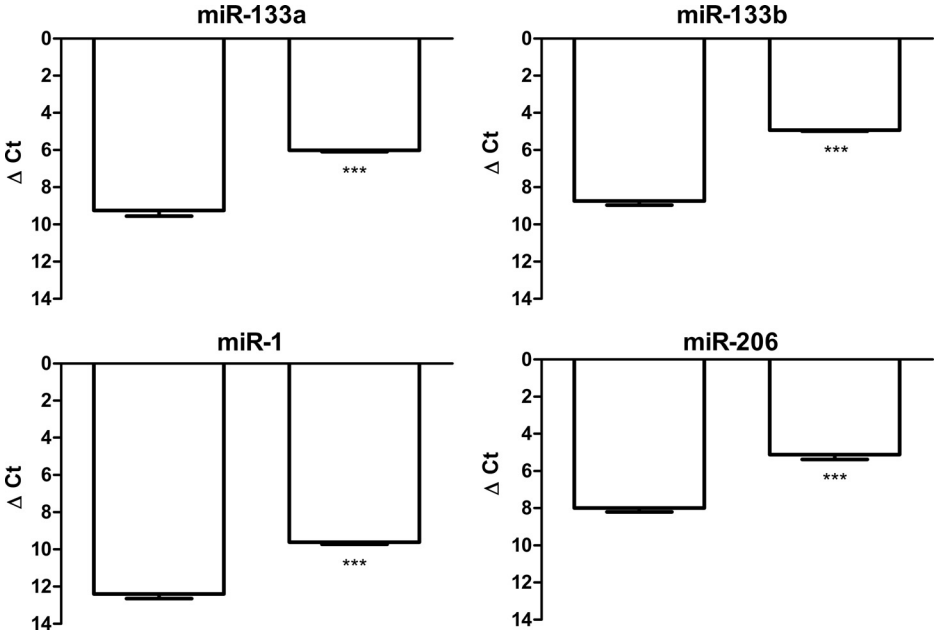

Fig. 9. Expression of miRNA. Pre-NMES to post-NMES relative expression (as ΔCt) of miR-133a, miR-133b, miR-1, and miR-206 (as indicated) in MPCs. Data are means ± SE from three independent experiments, each performed in triplicate. ***$P \leq 0.0001$.

cesses in the elderly, we investigated the redox balance of these pre-NMES and post-NMES MPCs. Surprisingly, the post-NMES MPCs showed significant reduction (~40%) in $O_2^{\cdot -}$ production even in the presence of increased number of MHC I fibers, which are the slow ones, those that rely mostly on mitochondrial oxidative metabolism.

Superoxide dismutase and glutathione peroxidase are the most important antioxidant enzymes for detoxification of $O_2^{\cdot -}$ and its derivative H_2O_2, respectively, but these did not show different activities between the pre-NMES and post-NMES MPCs. Moreover, the reduced trend of superoxide dismutase activity is in agreement with both the decreased $O_2^{\cdot -}$ production and the mitochondrial SOD2 protein reduction we found in post-NMES MPCs. Superoxide dismutase reduces $O_2^{\cdot -}$ to H_2O_2, which is then a substrate for glutathione peroxidase. In the present study, the glutathione peroxidase activity did not change. It might be that H_2O_2 that was also produced through oxygen reduction by other metabolic sources did not decrease with $O_2^{\cdot -}$, and as a consequence, the glutathione peroxidase activity of the post-NMES MPCs remained similar to that of the pre-NMES MPCs. In accordance, the data on general cellular peroxidation performed using DCF fluorescence revealed that the cellular peroxidation end products measured directly on cells did not vary between pre- and post-NMES. It may be that the period of 8 wk of stimulation was not sufficient to reduce the MPC general oxidative state in elderly subjects, as expected considering the $O_2^{\cdot -}$ reduction. From another point of view, it is also interesting that the general oxidation did not increase even in the presence of increased percentage of oxidative MHC I fiber, which confirms data on NMES-dependent atypical fiber adaptation already present in the literature (20). Moreover, it could be that the NMES protocol has to be performed with other strategies, such as active training, to reduce MPC general oxidation (4). Interestingly, the increased proportion of MHC I fibers at post-NMES along with reduced $O_2^{\cdot -}$ production and any increase of the oxidative status leads us to think that NMES could be a healthy treatment for the elderly.

The idea that miRNAs may regulate and be regulated by oxidative stress following active and/or passive exercise in skeletal muscle still awaits experimental validation. However, in other cellular models such as neurons, endothelial cells, and cardiomyocytes a specific miRNA regulation by oxidant level has been established (28, 35, 59). Yildirim et al. (60) demonstrated a relationship between increase of oxidative stress and downregulation of miR-1, miR-133a, and miR-133b in rat cardiomyocytes.

Recently, we demonstrated human regulation of miRNAs by $O_2^{\cdot -}$ production linked to low-intensity exercise. Indeed, we observed that human MPCs that decreased $O_2^{\cdot -}$ production showed upregulation of miR-1, miR-133b, and miR-206, whereas those that increased $O_2^{\cdot -}$ showed downregulation of these myo-miRNAs (34, 48).

Accordingly, the decreased $O_2^{\cdot -}$ production upregulated these myo-miRNAs, along with miR-133a, which promoted (or supported) the myogenesis process and confirmed the positive role of the NMES protocol.

Nakasa et al. (38) demonstrated that local injection of a miR-1, miR-133, and miR-206 mixture in rat skeletal muscle increased muscle regeneration via increased myogenic regulatory factors such as myogenin. Furthermore, upregulation of miR-1, miR-133a/b, and miR-206 might be linked to reduction of muscle inflammation (19), which would also be consistent with a reduction in the $O_2^{\cdot -}$ levels as a positive effect of the NMES protocol. Moreover, it has been demonstrated that miR-133 and miR-1 expression is linked to the regulation of apoptotic pathways (10). Although we did not obtain information about this specific pathway here, we believe that the upregulation of both miR-1 and miR-133a/b could be in line with apoptosis repression, in favor of cell proliferation (9, 24, 48).

One of the most important effects of stimulation of the skeletal muscle regeneration process, which in the present case relates to MPC fusion with myofibers, is the increased cross-sectional area and isometric strength of myofibers and, as a direct consequence, the increase in muscle strength. The iso-

metric maximal voluntary strength of lower limbs measured post-NMES significantly increased with respect to pre-NMES, in accordance with the present literature (11, 23). Interestingly, we found other positive NMES effects on elderly mobility, as revealed by FTSST and TUG functional tests. These effects reveal an important physiological outcome of this NMES-dependent activation of skeletal muscle regeneration and suggest that NMES may thus be further considered for counteracting sarcopenia. Indeed, even if one limitation of this method could be the discomfort that is associated with the intensity of the electrically induced muscle contractions (23, 31), in our experience, NMES has been well tolerated by elderly subjects. Moreover, NMES could be considered as an important adjuvant in a clinical approach for those individuals who are unable to exercise because of orthopedic problems or other complications, also considering the positive effect on energy expenditure and human metabolism enhancement reported in the literature (22, 49).

In conclusion, neuromuscular electrical stimulation is an interesting protocol for the stimulation of human skeletal muscle, even if this is achieved passively and in a localized manner. Although NMES is extensively used in sport and human muscle rehabilitation, there is little evidence of the physiological effects, and there are few data on regeneration of human sarcopenic muscle. We have demonstrated in the present study that NMES stimulates specific physiological signals for MPC regeneration, which can result in increased fusion of satellite cells with existing mature myofibers of the elderly through increases in $[Ca^{2+}]_{cyt}$. This process appears to be driven by overexpression of myogenin that is sustained by upregulation of myo-miRNAs, which can occur because of reduced $O_2^{\cdot -}$ production in the MPCs stimulated by this NMES protocol. In conclusion, NMES can help muscle regeneration and increase the maximal isometric strength of the lower limbs in healthy elderly subjects along with their mobility.

ACKNOWLEDGMENTS

We thank all of the subjects who volunteered to participate in this study for their collaboration. We thank Dr. Christopher Berrie for English editing.

GRANTS

This study was funded by G. d'Annunzio University grants to T. Pietrangelo, R. Mancinelli, and S. Fulle and Projects of National Interest (PRIN) National Grants 2007AWZTHH_003 to S. Fulle and 2012N8YJC3_003 to T. Pietrangelo.

DISCLOSURES

No conflicts of interest, financial or otherwise, are declared by the authors.

AUTHOR CONTRIBUTIONS

S.F. and T.P. conceived and designed research; E.S.D.F., R.M., M.M., C.D., V.V., L.T., J.L.D., and T.P. performed experiments; E.S.D.F., R.M., M.M., L.T., J.L.D., S.F., and T.P. analyzed data; E.S.D.F., R.M., S.F., and T.P. interpreted results of experiments; E.S.D.F., R.M., and T.P. prepared figures; E.S.D.F. and T.P. drafted manuscript; E.S.D.F., R.M., J.L.D., S.F., and T.P. edited and revised manuscript; E.S.D.F., R.M., M.M., C.D., V.V., L.T., J.L.D., S.F., and T.P. approved final version of manuscript.

REFERENCES

1. **Antigny F, Koenig S, Bernheim L, Frieden M.** During post-natal human myogenesis, normal myotube size requires TRPC1- and TRPC4-mediated Ca^{2+} entry. *J Cell Sci* 126: 2525–2533, 2013. doi:10.1242/jcs.122911.
2. **Antigny F, Konig S, Bernheim L, Frieden M.** Inositol 1,4,5 trisphosphate receptor 1 is a key player of human myoblast differentiation. *Cell Calcium* 56: 513–521, 2014. doi:10.1016/j.ceca.2014.10.014.
3. **Arnaudeau S, Holzer N, König S, Bader CR, Bernheim L.** Calcium sources used by post-natal human myoblasts during initial differentiation. *J Cell Physiol* 208: 435–445, 2006. doi:10.1002/jcp.20679.
4. **Baar K.** Using molecular biology to maximize concurrent training. *Sports Med* 44, *Suppl* 2: S117–S125, 2014. doi:10.1007/s40279-014-0252-0.
5. **Beccafico S, Puglielli C, Pietrangelo T, Bellomo R, Fanò G, Fulle S.** Age-dependent effects on functional aspects in human satellite cells. *Ann N Y Acad Sci* 1100: 345–352, 2007. doi:10.1196/annals.1395.037.
6. **Bijlenga P, Liu JH, Espinos E, Haenggeli CA, Fischer-Lougheed J, Bader CR, Bernheim L.** T-type alpha 1H Ca^{2+} channels are involved in Ca^{2+} signaling during terminal differentiation (fusion) of human myoblasts. *Proc Natl Acad Sci USA* 97: 7627–7632, 2000. doi:10.1073/pnas.97.13.7627.
7. **Bottinelli R, Canepari M, Pellegrino MA, Reggiani C.** Force-velocity properties of human skeletal muscle fibres: myosin heavy chain isoform and temperature dependence. *J Physiol* 495: 573–586, 1996. doi:10.1113/jphysiol.1996.sp021617.
8. **Ceafalan LC, Popescu BO, Hinescu ME.** Cellular players in skeletal muscle regeneration. *BioMed Res Int* 2014: 957014, 2014. doi:10.1155/2014/957014.
9. **Crippa S, Cassano M, Sampaolesi M.** Role of miRNAs in muscle stem cell biology: proliferation, differentiation and death. *Curr Pharm Des* 18: 1718–1729, 2012. doi:10.2174/138161212799859620.
10. **Di Filippo ES, Mancinelli R, Pietrangelo T, La Rovere RM, Quattrocelli M, Sampaolesi M, Fulle S.** Myomir dysregulation and reactive oxygen species in aged human satellite cells. *Biochem Biophys Res Commun* 473: 462–470, 2016. doi:10.1016/j.bbrc.2016.03.030.
11. **Filipovic A, Kleinöder H, Dörmann U, Mester J.** Electromyostimulation: a systematic review of the effects of different electromyostimulation methods on selected strength parameters in trained and elite athletes. *J Strength Cond Res* 26: 2600–2614, 2012. doi:10.1519/JSC.0b013e31823f2cd1.
12. **Fisher-Wellman K, Bloomer RJ.** Acute exercise and oxidative stress: a 30 year history. *Dyn Med* 8: 1, 2009. doi:10.1186/1476-5918-8-1.
13. **Franceschi C, Campisi J.** Chronic inflammation (inflammaging) and its potential contribution to age-associated diseases. *J Gerontol A Biol Sci Med Sci* 69, *Suppl* 1: S4–S9, 2014. doi:10.1093/gerona/glu057.
14. **Fujiya H, Ogura Y, Ohno Y, Goto A, Nakamura A, Ohashi K, Uematsu D, Aoki H, Musha H, Goto K.** Microcurrent electrical neuromuscular stimulation facilitates regeneration of injured skeletal muscle in mice. *J Sports Sci Med* 14: 297–303, 2015.
15. **Fulle S, Mecocci P, Fanó G, Vecchiet I, Vecchini A, Racciotti D, Cherubini A, Pizzigallo E, Vecchiet L, Senin U, Beal MF.** Specific oxidative alterations in vastus lateralis muscle of patients with the diagnosis of chronic fatigue syndrome. *Free Radic Biol Med* 29: 1252–1259, 2000. doi:10.1016/S0891-5849(00)00419-6.
16. **Fulle S, Di Donna S, Puglielli C, Pietrangelo T, Beccafico S, Bellomo R, Protasi F, Fanò G.** Age-dependent imbalance of the antioxidative system in human satellite cells. *Exp Gerontol* 40: 189–197, 2005. doi:10.1016/j.exger.2004.11.006.
17. **Fulle S, Pietrangelo T, Mancinelli R, Saggini R, Fanò G.** Specific correlations between muscle oxidative stress and chronic fatigue syndrome: a working hypothesis. *J Muscle Res Cell Motil* 28: 355–362, 2007. doi:10.1007/s10974-008-9128-y.
18. **Fulle S, Sancilio S, Mancinelli R, Gatta V, Di Pietro R.** Dual role of the caspase enzymes in satellite cells from aged and young subjects. *Cell Death Dis* 4: e955, 2013. doi:10.1038/cddis.2013.472.
19. **Georgantas RW, Streicher K, Greenberg SA, Greenlees LM, Zhu W, Brohawn PZ, Higgs BW, Czapiga M, Morehouse CA, Amato A, Richman L, Jallal B, Yao Y, Ranade K.** Inhibition of myogenic microRNAs 1, 133, and 206 by inflammatory cytokines links inflammation and muscle degeneration in adult inflammatory myopathies. *Arthritis Rheumatol* 66: 1022–1033, 2014. doi:10.1002/art.38292.
20. **Gondin J, Brocca L, Bellinzona E, D'Antona G, Maffiuletti NA, Miotti D, Pellegrino MA, Bottinelli R.** Neuromuscular electrical stimulation training induces atypical adaptations of the human skeletal muscle phenotype: a functional and proteomic analysis. *J Appl Physiol (1985)* 110: 433–450, 2011. doi:10.1152/japplphysiol.00914.2010.
21. **Guo BS, Cheung KK, Yeung SS, Zhang BT, Yeung EW.** Electrical stimulation influences satellite cell proliferation and apoptosis in unload-

ing-induced muscle atrophy in mice. *PLoS One* 7: e30348, 2012. doi:10.1371/journal.pone.0030348.
22. **Hamada T, Hayashi T, Kimura T, Nakao K, Moritani T.** Electrical stimulation of human lower extremities enhances energy consumption, carbohydrate oxidation, and whole body glucose uptake. *J Appl Physiol (1985)* 96: 911–916, 2004. doi:10.1152/japplphysiol.00664.2003.
23. **Herzig D, Maffiuletti NA, Eser P.** The application of neuromuscular electrical stimulation training in various non-neurologic patient populations: a narrative review. *PM R* 7: 1167–1178, 2015. doi:10.1016/j.pmrj.2015.03.022.
24. **Huang ZP, Espinoza-Lewis R, Wang DZ.** Determination of miRNA targets in skeletal muscle cells. *Methods Mol Biol* 798: 475–490, 2012. doi:10.1007/978-1-61779-343-1_28.
25. **Kadi F, Johansson F, Johansson R, Sjöström M, Henriksson J.** Effects of one bout of endurance exercise on the expression of myogenin in human quadriceps muscle. *Histochem Cell Biol* 121: 329–334, 2004. doi:10.1007/s00418-004-0630-z.
26. **Kvorning T, Kadi F, Schjerling P, Andersen M, Brixen K, Suetta C, Madsen K.** The activity of satellite cells and myonuclei following 8 weeks of strength training in young men with suppressed testosterone levels. *Acta Physiol (Oxf)* 213: 676–687, 2015. doi:10.1111/apha.12404.
27. **La Rovere RML, Quattrocelli M, Pietrangelo T, Di Filippo ES, Maccatrozzo L, Cassano M, Mascarello F, Barthélémy I, Blot S, Sampaolesi M, Fulle S.** Myogenic potential of canine craniofacial satellite cells. *Front Aging Neurosci* 6: 90, 2014. doi:10.3389/fnagi.2014.00090.
28. **Li R, Yan G, Li Q, Sun H, Hu Y, Sun J, Xu B.** MicroRNA-145 protects cardiomyocytes against hydrogen peroxide (H_2O_2)-induced apoptosis through targeting the mitochondria apoptotic pathway. *PLoS One* 7: e44907, 2012. doi:10.1371/journal.pone.0044907.
29. **Liu JH, König S, Michel M, Arnaudeau S, Fischer-Lougheed J, Bader CR, Bernheim L.** Acceleration of human myoblast fusion by depolarization: graded Ca^{2+} signals involved. *Development* 130: 3437–3446, 2003. doi:10.1242/dev.00562.
30. **Lorenzon P, Bandi E, de Guarrini F, Pietrangelo T, Schäfer R, Zweyer M, Wernig A, Ruzzier F.** Ageing affects the differentiation potential of human myoblasts. *Exp Gerontol* 39: 1545–1554, 2004. doi:10.1016/j.exger.2004.07.008.
31. **Maffiuletti NA.** Physiological and methodological considerations for the use of neuromuscular electrical stimulation. *Eur J Appl Physiol* 110: 223–234, 2010. doi:10.1007/s00421-010-1502-y.
32. **Mancinelli R, Pietrangelo T, La Rovere R, Toniolo L, Fanò G, Reggiani C, Fulle S.** Cellular and molecular responses of human skeletal muscle exposed to hypoxic environment. *J Biol Regul Homeost Agents* 25: 635–645, 2011.
33. **Mancinelli R, Pietrangelo T, Burnstock G, Fanò G, Fulle S.** Transcriptional profile of GTP-mediated differentiation of C2C12 skeletal muscle cells. *Purinergic Signal* 8: 207–221, 2012. doi:10.1007/s11302-011-9266-3.
34. **Mancinelli R, Di Filippo ES, Verratti V, Fulle S, Toniolo L, Reggiani C, Pietrangelo T.** The regenerative potential of female skeletal muscle upon hypobaric hypoxic exposure. *Front Physiol* 7: 303, 2016. doi:10.3389/fphys.2016.00303.
35. **Marin T, Gongol B, Chen Z, Woo B, Subramaniam S, Chien S, Shyy JY.** Mechanosensitive microRNAs-role in endothelial responses to shear stress and redox state. *Free Radic Biol Med* 64: 61–68, 2013. doi:10.1016/j.freeradbiomed.2013.05.034.
36. **Minetto MA, Botter A, Bottinelli O, Miotti D, Bottinelli R, D'Antona G.** Variability in muscle adaptation to electrical stimulation. *Int J Sports Med* 34: 544–553, 2013. doi:10.1055/s-0032-1321799.
37. **Muller FL, Liu Y, Van Remmen H.** Complex III releases superoxide to both sides of the inner mitochondrial membrane. *J Biol Chem* 279: 49064–49073, 2004. doi:10.1074/jbc.M407715200.
38. **Nakasa T, Ishikawa M, Shi M, Shibuya H, Adachi N, Ochi M.** Acceleration of muscle regeneration by local injection of muscle-specific microRNAs in rat skeletal muscle injury model. *J Cell Mol Med* 14: 2495–2505, 2010. doi:10.1111/j.1582-4934.2009.00898.x.
39. **Ohno Y, Fujiya H, Goto A, Nakamura A, Nishiura Y, Sugiura T, Ohira Y, Yoshioka T, Goto K.** Microcurrent electrical nerve stimulation facilitates regrowth of mouse soleus muscle. *Int J Med Sci* 10: 1286–1294, 2013. doi:10.7150/ijms.5985.
40. **Paoli A, Pacelli QF, Cancellara P, Toniolo L, Moro T, Canato M, Miotti D, Reggiani C.** Myosin isoforms and contractile properties of single fibers of human latissimus dorsi muscle. *BioMed Res Int* 2013: 249398, 2013. doi:10.1155/2013/249398.
41. **Pellegrino MA, Canepari M, Rossi R, D'Antona G, Reggiani C, Bottinelli R.** Orthologous myosin isoforms and scaling of shortening velocity with body size in mouse, rat, rabbit and human muscles. *J Physiol* 546: 677–689, 2003. doi:10.1113/jphysiol.2002.027375.
42. **Pietrangelo T, Fioretti B, Mancinelli R, Catacuzzeno L, Franciolini F, Fanò G, Fulle S.** Extracellular guanosine-5′-triphosphate modulates myogenesis via intermediate $Ca(^{2+})$-activated K^+ currents in C2C12 mouse cells. *J Physiol* 572: 721–733, 2006. doi:10.1113/jphysiol.2005.102194.
43. **Pietrangelo T, D'Amelio L, Doria C, Mancinelli R, Fulle S, Fanò G.** Tiny percutaneous needle biopsy: An efficient method for studying cellular and molecular aspects of skeletal muscle in humans. *Int J Mol Med* 27: 361–367, 2011. doi:10.3892/ijmm.2010.582.
44. **Pietrangelo T, Mariggiò MA, Lorenzon P, Fulle S, Protasi F, Rathbone M, Werstiuk E, Fanò G.** Characterization of specific GTP binding sites in C2C12 mouse skeletal muscle cells. *J Muscle Res Cell Motil* 23: 107–118, 2002. doi:10.1023/A:1020288117082.
45. **Pietrangelo T, Puglielli C, Mancinelli R, Beccafico S, Fanò G, Fulle S.** Molecular basis of the myogenic profile of aged human skeletal muscle satellite cells during differentiation. *Exp Gerontol* 44: 523–531, 2009. doi:10.1016/j.exger.2009.05.002.
46. **Pietrangelo T, Mancinelli R, Doria C, Di Tano G, Loffredo B, Fanò-Illic G, Fulle S.** Endurance and resistance training modifies the transcriptional profile of the vastus lateralis skeletal muscle in healthy elderly subjects. *Sport Sci Health* 7: 19–27, 2012. doi:10.1007/s11332-012-0107-8.
47. **Pietrangelo T, Perni S, Di Tano G, Fanò-Illic G, Franzini-Armstrong C.** A method for the ultrastructural preservation of tiny percutaneous needle biopsy material from skeletal muscle. *Int J Mol Med* 32: 965–970, 2013. doi:10.3892/ijmm.2013.1454.
48. **Pietrangelo T, Di Filippo ES, Mancinelli R, Doria C, Rotini A, Fanò-Illic G, Fulle S.** Low intensity exercise training improves skeletal muscle regeneration potential. *Front Physiol* 6: 399, 2015. doi:10.3389/fphys.2015.00399.
48a. **Podsiadlo D, Richardson S.** The timed "Up & Go": a test of basic functional mobility for frail elderly persons. *J Am Geriatr Soc* 39: 142–148, 1991.
49. **Porcelli S, Marzorati M, Pugliese L, Adamo S, Gondin J, Bottinelli R, Grassi B.** Lack of functional effects of neuromuscular electrical stimulation on skeletal muscle oxidative metabolism in healthy humans. *J Appl Physiol (1985)* 113: 1101–1109, 2012. doi:10.1152/japplphysiol.01627.2011.
50. **Powers SK, Duarte J, Kavazis AN, Talbert EE.** Reactive oxygen species are signalling molecules for skeletal muscle adaptation. *Exp Physiol* 95: 1–9, 2010. doi:10.1113/expphysiol.2009.050526.
51. **Quinlan CL, Perevoshchikova IV, Hey-Mogensen M, Orr AL, Brand MD.** Sites of reactive oxygen species generation by mitochondria oxidizing different substrates. *Redox Biol* 1: 304–312, 2013. doi:10.1016/j.redox.2013.04.005.
52. **Sciancalepore M, Coslovich T, Lorenzon P, Ziraldo G, Taccola G.** Extracellular stimulation with human "noisy" electromyographic patterns facilitates myotube activity. *J Muscle Res Cell Motil* 36: 349–357, 2015. doi:10.1007/s10974-015-9424-2.
53. **Shakirzyanova A, Valeeva G, Giniatullin A, Naumenko N, Fulle S, Akulov A, Atalay M, Nikolsky E, Giniatullin R.** Age-dependent action of reactive oxygen species on transmitter release in mammalian neuromuscular junctions. *Neurobiol Aging* 38: 73–81, 2016. doi:10.1016/j.neurobiolaging.2015.10.023.
54. **Snijders T, Verdijk LB, Beelen M, McKay BR, Parise G, Kadi F, van Loon LJ.** A single bout of exercise activates skeletal muscle satellite cells during subsequent overnight recovery. *Exp Physiol* 97: 762–773, 2012. doi:10.1113/expphysiol.2011.063313.
55. **Sullivan-Gunn MJ, Lewandowski PA.** Elevated hydrogen peroxide and decreased catalase and glutathione peroxidase protection are associated with aging sarcopenia. *BMC Geriatr* 13: 104, 2013. doi:10.1186/1471-2318-13-104.
55a. **Talmadge RJ, Roy RR.** Electrophoretic separation of rat skeletal muscle myosin heavy-chain isoforms. *J Appl Physiol (1985)* 75: 2337–2340, 1993.
56. **Toniolo L, Maccatrozzo L, Patruno M, Pavan E, Caliaro F, Rossi R, Rinaldi C, Canepari M, Reggiani C, Mascarello F.** Fiber types in canine muscles: myosin isoform expression and functional characterization. *Am J Physiol Cell Physiol* 292: C1915–C1926, 2007. doi:10.1152/ajpcell.00601.2006.
57. **Verdijk LB.** Satellite cell activation as a critical step in skeletal muscle plasticity. *Exp Physiol* 99: 1449–1450, 2014. doi:10.1113/expphysiol.2014.081273.

58. **Whitney SL, Wrisley DM, Marchetti GF, Gee MA, Redfern MS, Furman JM.** Clinical measurement of sit-to-stand performance in people with balance disorders: validity of data for the five-times-sit-to-stand test. *Phys Ther* 85: 1034–1045, 2005.
59. **Xu S, Zhang R, Niu J, Cui D, Xie B, Zhang B, Lu K, Yu W, Wang X, Zhang Q.** Oxidative stress mediated-alterations of the microRNA expression profile in mouse hippocampal neurons. *Int J Mol Sci* 13: 16945–16960, 2012. doi:10.3390/ijms131216945.
60. **Yildirim SS, Akman D, Catalucci D, Turan B.** Relationship between downregulation of miRNAs and increase of oxidative stress in the development of diabetic cardiac dysfunction: junctin as a target protein of miR-1. *Cell Biochem Biophys* 67: 1397–1408, 2013. doi:10.1007/s12013-013-9672-y.